Muon-spin-rotation studies of $HoNi_2B_2C$

L. P. Le, R. H. Heffner, and J. D. Thompson
Los Alamos National Laboratory, Los Alamos, New Mexico 87545

D. E. MacLaughlin
University of California, Riverside, California 92521

G. J. Nieuwenhuys
Kamerlingh Onnes Laboratory, Leiden University, P.O. Box 9506, 2300 RA Leiden, The Netherlands

A. Amato, R. Feyerherm, F. N. Gygax, and A. Schenck
Institute for Particle Physics, Eidgenössische Technische Hochschule Zurich, CH-5232 Villigen PSI, Switzerland

P. C. Canfield and B. K. Cho
Ames Laboratory and Department of Physics and Astronomy, Iowa State University, Ames, Iowa 50011
(Received 30 May 1995; revised manuscript received 10 October 1995)

Muon-spin-rotation and relaxation studies on single-crystalline $HoNi_2B_2C$ show two magnetic phase transitions at $T_{N1}=6.0$ K and at $T_{N2}=5.0$ K. While the low-temperature phase displays a commensurate antiferromagnetic structure, the higher-temperature phase exhibits an incommensurately sinusoidal modulation of the spin amplitude. The nature of the incommensurate state, along with the causes of the reentrant superconductivity near 5 K, are discussed.

The interplay and competition between superconductivity and magnetism has been an important subject in the study of condensed-matter physics for more than two decades. In the late 1970s and early 1980s ternary compounds such as $R\mathrm{Rh}_4\mathrm{B}_4$ and $R\mathrm{Mo}_6\mathrm{S}_8$ (R=rare earth) were found to exhibit either ferromagnetic (FM) or antiferromagnetic (AFM) phases which occur below the superconducting transition temperature and which destroy or coexist with the superconducting phase, respectively.[1,2] The most recently discovered examples of magnetic superconductors are the rare-earth quaternary borocarbide materials $RM_2\mathrm{B}_2\mathrm{C}$, where M=Ni or Pt.[3–8] These materials exhibit a superconducting transition temperature T_c as high as 16.6 K (for $LuNi_2B_2C$) and, with the substitution of magnetic rare earths, exhibit coexistence of antiferromagnetism and superconductivity.

Among the heavy rare-earth $R\mathrm{Ni}_2\mathrm{B}_2\mathrm{C}$ compounds, the substitution of magnetic ions enhances the Néel temperature T_N and depresses T_c monotonically, following the rare-earth ion de Gennes factor.[6,9] Except for Gd and Tb, with the largest de Gennes factors, superconductivity is not quenched completely. This is consistent with a relatively weak coupling between the superconducting and rare-earth electrons, similar to the situation found in $R\mathrm{Rh}_4\mathrm{B}_4$ and $R\mathrm{Mo}_6\mathrm{Se}_8$. For R=Ho, Er, and Tm, the upper critical field and resistivity curves[6,8,10,11] exhibit a tendency toward reentrant normal-state behavior below T_c, depending upon the applied field. This tendency is particularly clear for R=Ho, where reentrance is found in zero[6] or low applied magnetic fields.[8] Recent neutron-scattering experiments[12,13] on $HoNi_2B_2C$ observed an incommensurate magnetic structure around 5 K, which was interpreted as facilitating the reentrant behavior. Here we report muon-spin-rotation and relaxation (μSR) studies on single-crystalline $HoNi_2B_2C$. The main points which these studies address are the nature of the incommensurate magnetic state near 5 K and the causes of the reentrant superconductivity in low fields. We find that the incommensurate state is inconsistent with the single spiral spin modulation proposed in Ref. 13; and our data indicate rather multiple-spiral modulation or incommensurate spin amplitude modulation.

The μSR experiments were performed at the Paul Scherrer Institute (PSI) in Villigen, Switzerland. The single-crystalline samples were prepared via the Ames Laboratory Ni_2B flux growth method, as described in Ref. 7, and are from similar growth batches as the single crystals used in the neutron-scattering measurements reported in Ref. 12. A mosaic of about ten crystals, each having a typical dimension of $4\times4\times0.5$ mm^3 and its crystallographic c axis perpendicular to the largest sample surface, were glued on a silver plate, so that the total sample covered an area of about 15×15 mm^2. About 10% of the muon beam stopped in the Ag backing, which produces negligible muon-spin relaxation. The remainder stopped in the sample material. The c axes of the crystals were aligned to within a few degrees; no attempt was made to align the crystals in the a-b plane.

Zero-field (ZF) μSR has been used extensively to investigate magnetic systems, because one can simultaneously study both the static and the dynamic magnetic properties.[14] In our preliminary analysis, ZF spectra were fit with a relaxation function given by

$$G(t)=A_1\cos(2\pi\nu t+\phi)\exp(-\lambda_1 t)+A_2\exp(-\lambda_2 t), \qquad (1)$$

where A_1 and A_2 are the spectral weights ($A_1+A_2=1$), ν is the muon precession frequency, and λ_1 and λ_2 are the damping rates for the oscillating and nonoscillating terms, respectively. Equation (1) corresponds to the case of a unique muon

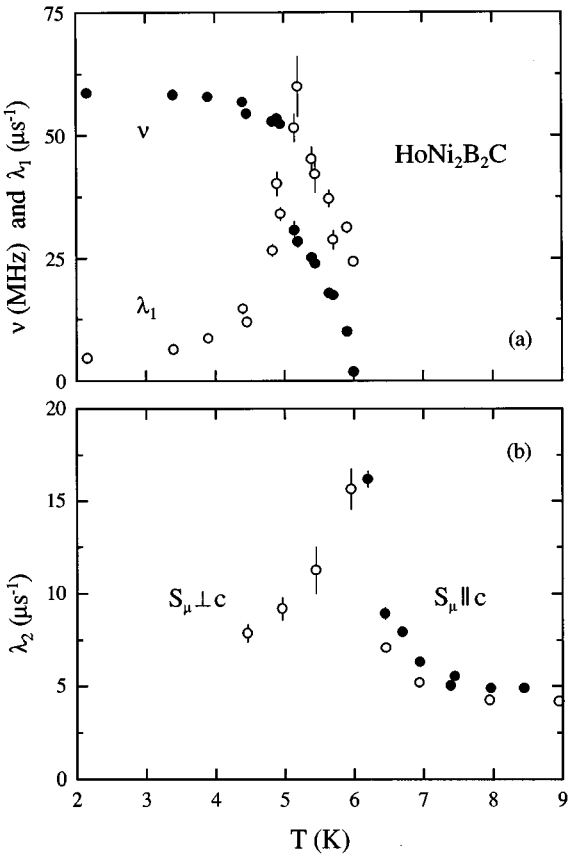

FIG. 1. Temperature dependence of ZF μSR (a) precession frequency and relaxation rates λ_1 for $\mathbf{S}_\mu \| c$, and (b) dynamic relaxation rate λ_2 in the single-crystalline $HoNi_2B_2C$. Two magnetic phase transitions are found at $T_{N1}=6.0$ K and $T_{N2}=5.0$ K.

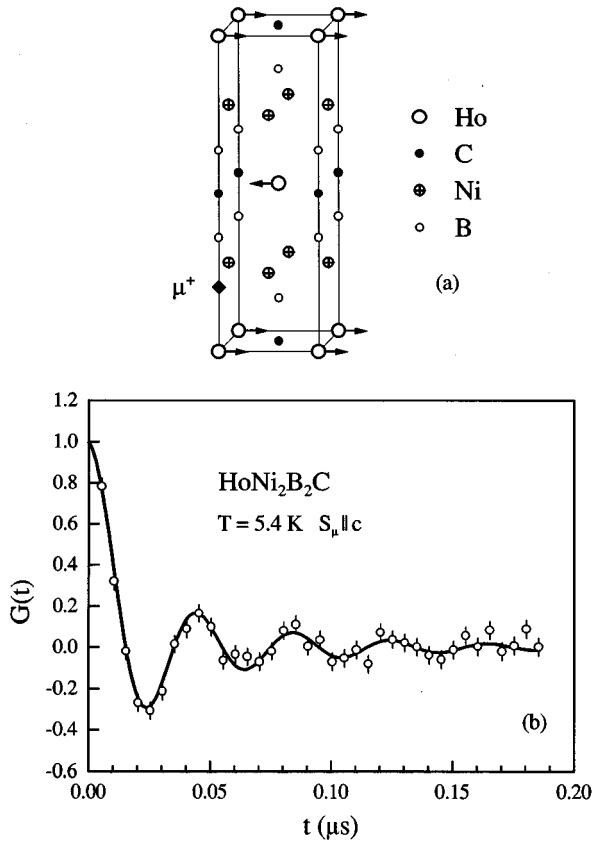

FIG. 2. (a) Crystal and magnetic structure below 5 K in $HoNi_2B_2C$. The solid diamond denotes the muon location. (b) ZF-μSR relaxation function $G(t)$ at 5.4 K in the single-crystalline $HoNi_2B_2C$. Solid curve denotes a fit to Eq. (3).

lattice site. The spectral weights are determined by the angle ϕ between the initial muon spin $\mathbf{S}_\mu$ and the internal field $\mathbf{B}_\mu$ at the muon site, such that $A_1=\sin^2\phi$ and $A_2=\cos^2\phi$. The frequency is proportional to B_μ, and hence also proportional to the sublattice magnetization M for an AFM. Both inhomogeneous broadening and spin dynamics contribute to λ_1, while λ_2 reflects solely the properties of the host spin fluctuations and is analogous to the spin-lattice relaxation rate $(1/T_1)$ in nuclear magnetic resonance (NMR).

ZF measurements were carried out in two configurations, with the initial muon spin either parallel or perpendicular to the c axis. The observation of a full-amplitude oscillation $(A_1=1)$ for $\mathbf{S}_\mu \| c$ below 6 K means that the muon local field is in the basal plane in the AFM state. This is also consistent with the finding that $A_1 \approx A_2 = 1/2$ for $\mathbf{S}_\mu \perp c$. The temperature dependences of the frequency and the relaxation rates are given in Fig. 1. The temperature dependence of ν in zero applied field indicates two magnetic phase transitions at $T_{N1}=6.0(1)$ K and $T_{N2}=5.0(1)$ K. Below T_{N2} the small ratio of $\lambda_1/2\pi\nu$ ($\leqslant 0.04$ for $T \leqslant 4.5$ K) indicates a rather uniform internal field, as expected for a commensurate AFM ground state. Below 4 K the frequency displays very weak temperature variation; in fact, our previous measurements on polycrystalline samples[15] showed that the frequency increases smoothly by only 2% as the temperature decreases from 4 to 0.1 K. The change of frequency near T_{N2} is rather rapid. Whether this indicates a first-order transition or a rather fast second-order transition is not clear from these data. While both ν and λ_1 display nearly the same T dependence in both configurations (for clarity only the results for $\mathbf{S}_\mu \| c$ are shown), λ_2 displays anisotropy above T_{N1}, with λ_2 for $\mathbf{S}_\mu \| c$ being about 15% larger than that for $\mathbf{S}_\mu \perp c$. The latter suggests slower magnetic fluctuations in the basal plane, consistent with a large in-plane susceptibility.[8] The most interesting result obtained concerns the nature of the second magnetic phase between $T_{N1}=6.0$ K and $T_{N2}=5.0$ K (hereafter phase I). In the following, we first establish the muon lattice site, then discuss the magnetic behavior of phase I.

It is known that $HoNi_2B_2C$ has a body-centered-tetragonal structure, and the Ho moments are antiferromagnetically aligned below T_{N2},[5,8,12] as shown in Fig. 2(a). By symmetry we can narrow down the possible muon sites. Considering that only one frequency is observed and the muon local field is in the basal plane (see above), our numerical calculations show that the only possible sites are the axially symmetric site $(0,0,z)$ and the basal plane site $(x,x,0)$. However, at the $(x,x,0)$ site the calculated muon local field is at least an order of magnitude larger than observed, leaving the $(0,0,z)$ site. To determine the value of z, Knight shift measurements[14] with an applied field $H_0=5$ kOe were carried out. With the axially symmetric crystal structure and muon site, the observed susceptibility $\chi(\theta)$ and Knight shift $K(\theta)$ can be expressed as

$$\chi(\theta)=\chi_{\parallel}\cos^2\theta+\chi_{\perp}\sin^2\theta,$$

$$K(\theta)=K_c+A_{\rm thf}(\chi_{\parallel}\cos^2\theta+\chi_{\perp}\sin^2\theta)+A_{\rm dip}\left(\chi_{\parallel}\cos^2\theta-\frac{1}{2}\chi_{\perp}\sin^2\theta\right)+K_{\rm Ld}, \qquad (2)$$

where θ is the angle between $\mathbf{H}_0$ and the c axis, K_c is the shift due to conduction electrons (assumed to be isotropic), $A_{\rm thf}$ is the transferred hyperfine coupling constant (also assumed isotropic) between the muon and the anisotropic f susceptibility, $A_{\rm dip}$ describes the muon/f-moment dipolar coupling, and $K_{\rm Ld}$ describes the known Lorentz and demagnetizing fields. Using two sets of high-temperature data (χ,K) with $\theta=0°$ and $\theta=45°$ for $T\geqslant 70$ K, we find that $A_{\rm dip}=2.03(7)$ kOe/μ_B, $A_{\rm thf}=0.15(2)$ kOe/μ_B, and $K_c=-0.11(4)\%$. From the dominant coupling $A_{\rm dip}$ we determine the muon location $\mathbf{R}_\mu=(0,0,0.20)$, which is in a cavity surrounded by B, Ho, and four Ni atoms, as indicated in Fig. 2(a). This muon site is further confirmed by calculating the resultant ground-state moment from ν in zero external field below T_{N2}, assuming no change of $A_{\rm thf}$ between $H_0=0$ and 5 kOe. We find 11 ± 1.5 μ_B/Ho, which is consistent with the neutron-scattering results.[12]

We now discuss the nature of the magnetic phase I. Because the Ho moments are in the basal plane and the dipolar field at $\mathbf{R}_\mu$ is dominated by the spin at the origin, the magnetic field is approximately proportional to the spin, and therefore the field distribution is essentially the same as the spin distribution. For instance, a spiral modulation of the Ho spins (with a constant spin amplitude) would yield a spiral field distribution with nearly uniform amplitude, depending only weakly on the wave vector $\mathbf{Q}$. Thus, the magnitude of the field distribution for a spiral would be similar to that observed in the commensurate AFM state. This is likely to be the case for $ErNi_2B_2C$, where we have observed a rather uniform muon internal field ($\lambda_1/2\pi\nu=0.03$ at 3 K),[16] despite an incommensurate magnetic structure below $T_N=6$ K.[17] In contrast, an incommensurate modulation of the spin amplitude (IMSA) in $HoNi_2B_2C$ would yield a broad field distribution. The simplest IMSA with $\mathbf{S}_n=\mathbf{S}_0\cos(\mathbf{Q}\cdot\mathbf{R}_n)$ has a sinusoidal spin distribution $\rho(S)=(1/\pi)(S_0^2-S^2)^{-1/2}$, which in turn leads to a Bessel function $J_0(2\pi\nu t)$ for $G(t)$, where ν is the peak frequency corresponding to the maximum spin amplitude S_0.[18] The observed $G(t)$ in phase I of single-crystalline $HoNi_2B_2C$ is in fact best described by a damped Bessel function

$$G(t)=J_0(2\pi\nu t)\exp(-\lambda t), \qquad (3)$$

as shown in Fig. 2(b). At $T=5.4$ K, we have $\nu=25$ MHz and $\lambda=13$ μs^{-1}. The damping rate λ is attributed to dynamic relaxation, since $\lambda\approx\lambda_2$. A nearly constant ratio of λ_1/ν between T_{N2} and T_{N1} [Fig. 1(a)] indicates no change of the line shape, and therefore, the spin amplitude in phase I is consistent with a sinusoidal modulation. The IMSA has been previously also found in the metallic Tm.[19]

Neutron studies have proposed either one[13] or two[12] incommensurate modulations in phase I. In both cases, spiral spin structures were proposed, although to our knowledge these experiments could *not* rule out our IMSA structures. As noted previously, a single spiral modulation would yield a relatively uniform field at the muon site, in contrast to our observation. Thus, if only a single modulation exists, it must be an IMSA, inconsistent with Ref. 13. In the case of two modulations, with one along the c axis and another along the a axis,[12] the nature of phase I depends on whether these two states are spatially separated or coexist locally; this is not clear at the moment. In the former case, both modulations would have to be of the IMSA type, with the spin amplitudes being roughly the same, thus yielding the same sinusoidal field distributions in both domains. In the latter case, two coexisting spirals (superposition) yield the same spin distribution as a single IMSA, if both spirals have the same amplitude. Other possible combinations of spiral and IMSA would generally yield a different spin distribution. For instance, two coexisting IMSA's lead to a much faster-damped oscillation in the relaxation function.[20] We thus conclude that the two incommensurate modulations in phase I are most likely two spirals (if spatially coexisting) or two IMSA's (if spatially separated), with roughly the same spin amplitudes.

TABLE I. Incommensurate AFM in $HoNi_2B_2C$ and $ErNi_2B_2C$.

Parameters	$HoNi_2B_2C$	$ErNi_2B_2C$
T_c	8 K [a]	10.5 K [b]
T_N	5 K and 6 K [a]	6 K [b]
Incommensurate state	5–6 K [a]	$\leqslant$6 K [b]
Wave vector	$Q_a=0.585$ [a]	$Q_a=0.553$ [b]
	$Q_c=0.915$ [a]	
$\lambda_1/2\pi\nu$	0.30	0.03
λ_2 at 5.5 K	12 μs^{-1}	1 μs^{-1}
$H_{c2}(0)$	2 kOe [c]	14–18 kOe [d]
Depth of minimum in H_{c2}	1 kOe [c]	0.5–2 kOe [d]
Normalized depth in H_{c2}	0.8–1.0 [c]	$\leqslant$0.15 [d]

[a]Reference 12.
[b]Reference 17.
[c]Reference 8.
[d]Reference 10.

The temperature range over which the magnetic phase I is observed clearly corresponds to the deep minimum observed[8,12] in the temperature dependence of the upper critical field H_{c2}. It was therefore concluded from neutron-scattering experiments[12,13] that the incommensurate magnetic phases cause the near reentrant behavior in $HoNi_2B_2C$. However, we argue that the incommensurate AFM state is not necessarily more destructive to superconductivity than the commensurate one, since the incommensurate wavelength $\delta=2\pi/Q$ is much smaller than the superconducting coherence length ξ for $HoNi_2B_2C$ [$\delta_c\approx 11.5$ Å and $\delta_a\approx 6.0$ Å,[12] and $\xi\approx 400$ Å (Ref. 6)]. Thus the AFM molecular field is averaged out over a range of order ξ. This is supported by neutron studies on $ErNi_2B_2C$,[17] where the magnetic structure is found to be incommensurate over the entire temperature range below T_N. In this system, not only does superconductivity survive at the lowest temperatures, but the minimum in H_{c2} is not particularly deep in comparison with the commensurate AFM superconductors, such as $Tb_{1.2}Mn_6S_8$.[21]

What then accounts for the difference between $HoNi_2B_2C$ and $ErNi_2B_2C$? In Table I we give a brief comparison of their properties. One sees that, compared to

$ErNi_2B_2C$, the Ho system displays: (1) two incommensurate AFM states (with $\mathbf{Q}_a$ and $\mathbf{Q}_c$) and (2) two magnetic transitions (at T_{N1} and T_{N2}), with the transition at T_{N2} being very sharp. Finally, one notes that (3) $H_{c2}(0)$ is much smaller in the Ho than in the Er system, while the depth of the minimum in H_{c2} is roughly comparable in the two systems. These facts can be qualitatively discussed within the context of models[22] developed earlier for other classes of rare-earth based AFM superconductors, such as RMo_6S_8 and RRh_4B_4. The principal theoretical finding is that AFM order (with $\mathbf{Q}=\mathbf{Q}_{\mathrm{AFM}}$) in the localized $4f$ spin system modifies the conduction-electron band structure, in such a way as to reduce the electron-phonon interaction between Cooper pairs because of a decreased probability of finding two electrons with opposite spins at the same site.[23] Furthermore, the s-f coupling can induce a spin-density wave in the conduction-electron system with wave vector $\mathbf{Q}_{\mathrm{AFM}}$, which is strongly enhanced when nesting occurs. Thus the superconducting order parameter is reduced on that piece of the Fermi surface which is nested with $\mathbf{Q}_{\mathrm{AFM}}$. These effects lead to increased pair breaking above the Abrikosov-Gor'kov value for elastic scattering from paramagnetic ions, and in particular a sudden decrease in H_{c2} below the onset of AFM order. (Inelastic scattering from AFM spin waves at $T \ll T_N$ can lead to additional pair breaking.) We therefore suggest that the large difference in $H_{c2}(0)$ between $HoNi_2B_2C$ and $ErNi_2B_2C$ is due to the existence of *two* incommensurate AFM states in the Ho system. This would be particularly true if a relatively large area of the Fermi surface is nested along the c axis in Ho, thus producing a larger pair-breaking effect and lowering $H_{c2}(0)$ substantially. Similarly, the strong pair-breaking effect in the Ho system could also result in a relatively deep dip in H_{c2}, i.e., the superconducting state reentering to the normal state near 5 K. The above Fermi-surface-nesting picture is supported by calculation of the generalized susceptibility in RNi_2B_2C,[24] which exhibits maxima at both $\mathbf{Q}_a$ and $\mathbf{Q}_c$. Finally, we note that Zarestky *et al.* have also suggested[17] that the c-axis modulation might lead to reentrance in $HoNi_2B_2C$, and that Cho *et al.*[10] have pointed out that it is perhaps the small $H_{c2}(0)$ in Ho which is relevant to its reentrance. It is also possible that the dynamical pair breaking might be different in the two systems, because we find that the muon-spin lattice relaxation rates differ by an order of magnitude, indicating much slower Ho-ion fluctuation rates compared to Er.

In conclusion, we have performed μSR experiments to investigate the magnetic properties of $HoNi_2B_2C$. Our analysis of μSR spectra indicates that the incommensurate structure between 5 and 6 K has a sinusoidal modulation of the spin amplitude. We further conclude that this state must be either two IMSA's or two spirals, depending on whether these two states are spatially separated or locally coexisting. We note that the two spirals are consistent with the neutron studies on the single-crystal samples,[12] but conflict with the results on the polycrystalline samples.[13] This is not surprising because the samples we used for μSR are from the same batch as those used for Ref. 12. Recent investigations also show that the neutron studies on powder suffered greatly from sample-to-sample irreproducibility.[25] A discussion of the difference between two neutron studies can be found in the recent comment by Vogt *et al.* and the reply by Grigereit *et al.*[26] Also of particular interest in this system is the strong pair-breaking process, which leads to reentrant behavior in the superconducting state. We have discussed several possible mechanisms for this phenomena. We think that a complementary study of two incommensurate AFM superconductors $HoNi_2B_2C$ and $ErNi_2B_2C$ may give clues for the further understanding of these new magnetic superconductors.

Work at Los Alamos was performed under the auspices of USDOE, and UC Riverside was supported in part by the USNSF (DMR-9114911). Ames Laboratory is operated for the USDOE by Iowa State University under Contract No. W-7405-ENG-82.

[1] See *Superconductivity in Ternary Compounds II*, edited by M. B. Maple and Ø. Fischer (Springer, Berlin, 1982).
[2] Ø. Fischer, *Magnetic Superconductors in Ferromagnetic Materials*, edited by E. P. Wohlfarth (North-Holland, Amsterdam, 1990), Vol. 5.
[3] R. Nagarajan *et al.*, Phys. Rev. Lett. **72**, 274 (1994).
[4] R. J. Cava *et al.*, Nature **367**, 146 (1994); **367**, 252 (1994).
[5] T. Siegrist *et al.*, Nature **367**, 254 (1994).
[6] H. Eisaki *et al.*, Phys. Rev. B **50**, 647 (1994).
[7] Ming Xu *et al.*, Physica C **227**, 321 (1994).
[8] P. C. Canfield *et al.*, Physica C **230**, 397 (1994); K. D. D. Rathnayaka *et al.* (unpublished).
[9] B. K. Cho *et al.*, Phys. Rev. B **52**, R3844 (1995); M. El Massalami *et al.*, Physica C **244**, 41 (1995).
[10] B. K. Cho *et al.*, Phys. Rev. B **52**, 3684 (1995).
[11] B. K. Cho *et al.*, Phys. Rev. B **52**, 3676 (1995).
[12] A. I. Goldman *et al.*, Phys. Rev. B **50**, 9668 (1994).
[13] T. E. Grigereit *et al.*, Phys. Rev. Lett. **73**, 2756 (1994).
[14] A. Schenck, *Muon Spin Rotation Spectroscopy* (Adam Hilger, Bristol, 1985).
[15] L. P. Le *et al.*, Physica B **206-207**, 552 (1995).
[16] L. P. Le *et al.* (unpublished).
[17] J. Zarestky *et al.*, Phys. Rev. B **51**, 678 (1995).
[18] L. P. Le *et al.*, Phys. Rev. B **48**, 7284 (1993).
[19] T. O. Brun *et al.*, Phys. Rev. Lett. **23**, 1295 (1969).
[20] D. E. MacLaughlin *et al.*, Phys. Rev. B **23**, 1039 (1981).
[21] M. Ishikawa and Ø. Fisher, Solid State Commun. **24**, 747 (1977).
[22] K. Machida *et al.*, Phys. Rev. B **22**, 2307 (1980); K. Machida *et al.*, Phys. Rev. Lett. **44**, 821 (1980); M. J. Nass *et al.*, *ibid.* **46**, 614 (1981); T. V. Ramakrishnan and C. M. Varma, Phys. Rev. B **24**, 137 (1981).
[23] P. Fulde and G. Zwicknagl, J. Appl. Phys. **53**, 8064 (1982).
[24] Joo Yull Rhee *et al.*, Phys. Rev. B **51**, 15 585 (1995).
[25] P. C. Canfield *et al.* (private communication).
[26] T. Vogt *et al.*, Phys. Rev. Lett. **75**, 2628 (1995); T. E. Grigereit *et al.*, *ibid.*, 2629 (1995).